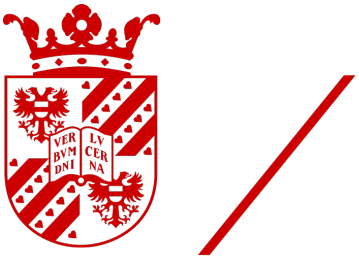

rijksuniversiteit
groningen

Bachelor Research Project: Exploring QCD-like theories with varying spacetime dimensions

Pablo Herrero Gómez
Supervisor: Prof. dr. Elisabetta Pallante
Second supervisor: Prof. dr. Rob Timmermans

June 2016

Contents

1 Introduction

In this paper we will review and discuss the properties and implications of the beta function structure for non-Abelian gauge theories, considering the conventional different limits for the number of fermions, N_f, and colors, N, as well as decreasing the number of spacetime dimensions from $d = 3 + 1$ using the ϵ expansion. We start (section 2.1) by reviewing 't Hooft large-N limit (so-called planar limit) and we explore its charm for string theory in $d = 1 + 1$ (section 2.2). After that, in section 2.3, and parallelly to the analysis performed for QED in [1], we discuss the existence of possible Wilson-Fisher (infrared) fixed points, in this same large-N limit, and higher dimensions[1] $1 + 1 < d < 3 + 1$. Similarities and differences with QED will also be further explored in section 3. In section 4, we shift the approach by continuously increase the number of fermions, N_f, exploring the phenomenological consequences of having N_f much smaller or much greater than N, or both quantities comparably large. In particular, the concepts of asymptotic and infrared freedom, UV and IR fixed points and asymptotic safety are reviewed (section 4.1) and the study of the beta function's derivative evaluated at the extrema is used to predict such behaviors (section 4.2). In section 4.3 we double-check the results in sections 2.3 and 3 by applying the previous analysis of the beta function. Finally, in section 5 we will leave aside dimensional variation to focus on a generalization of the theory in order to generate non-trivial UV fixed points in $d = 3 + 1$: the inclusion of Yukawa-like interactions. Following the recent article [2], we will first review asymptotic safety and the expansion of the running coupling constants in the vicinity of the UVFP (section 5.1). Then we will introduce the Veneziano limit (large N and N_f with fixed and small ratio N_f/N) in order to remain in the perturbative regime and we will study fixed points in a space with two parameters (in our case, couplin constants) in gauge-Yukawa theories as well as the stability matrix, its eigenvalues and eigendirections (section 5.2). We conclude by summarizing the main results and conclusions in section 6

2 't Hooft limit

2.1 Planar diagrams

Gerard 't Hooft introduced in 1973 the concept of planar diagrams [3]. This paper shows how, by sending N to infinity and the gauge coupling g to zero

[1] From now on we refer to the range $1+1 < d < 3+1$ as "higher dimensions". The case $d > 3 + 1$ will not be considered in this paper.

while keeping the product[2] $\lambda_t = g^2 N$ fixed and small, Feynman diagrams' leading contribution in $1/N$ is topologically planar.

To see this we use the double line notation for Feynman diagrams containing gluons. In this notation it is more convenient to treat the gluon field as a $N \times N$ matrix with two indices in the N and $\overline{N}$ representations:

$$(A_\mu)^i_j \equiv A^a_\mu (t_a)^i_j$$

where $(t_a)^i_j$ are the basis matrices of the Lie Algebra obeying $[t^a, t^b] = i f^{abc} t^c$, and f^{abc} the totally antisymmetric structure constant of the Lie Group.

Consider for example a three-loop (containing a three-vertex, V_3) vacuum diagram as in figure 2.1. The border quark lines close the diagram and tessellate the figure and each gluon propagator is represented as a double line following the two indices in the $N \times N$ representation.

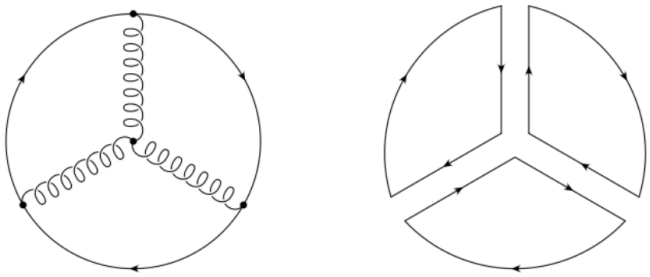

Figure 2.1: 3-loop vacuum diagram in double line notation. Courtesy of [4]

Diagrams such as this one are closed (they do not contain external lines) and associated with a factor

$$r = g^{V_3 + 2V_4} N^I$$

where I is the number of color index loops [3] and V_n is the number of n-point gluon vertices. An example of a three-point vertex, $n = 3$, is contained in figure 2.1 and a four-point vertex, $n = 4$, is shown in figure 2.2. Counting the number of internal lines or edges, E, we find the relation $2E = 3V_3 + 4V_4$, so we can manipulate the expression above to obtain

$$r = g^{2(E-V)} N^I = \lambda_t^{V-E} N^{V-E+I}$$

[2] We will use te subindex t for the 't Hooft parameter λ_t in order to distinguish it from the quartic self-interaction coefficient $\lambda\phi^4$ in section 2.3

[3] each of which raise a factor $\sum_{i=1}^{N} \delta^i_i$

where $V = V_3 + V_4$ is the total number of vertices and we have used 't Hooft parameter $\lambda_t = g^2 N$. The exponent of N can be written, using Euler's theorem [5], as

$$V - E + I = \chi = 2 - 2h - b$$

where b is the number of boundaries or quark loops and h is the genus of the Riemann surface (following the notation in [6]) with which we can associate these diagrams. Two differently connected examples are given in figure 2.2. Since h contributes as a negative power of N, the leading diagrams in $1/N$ must have $h = 0$, i.e. they are associated with planar diagrams.

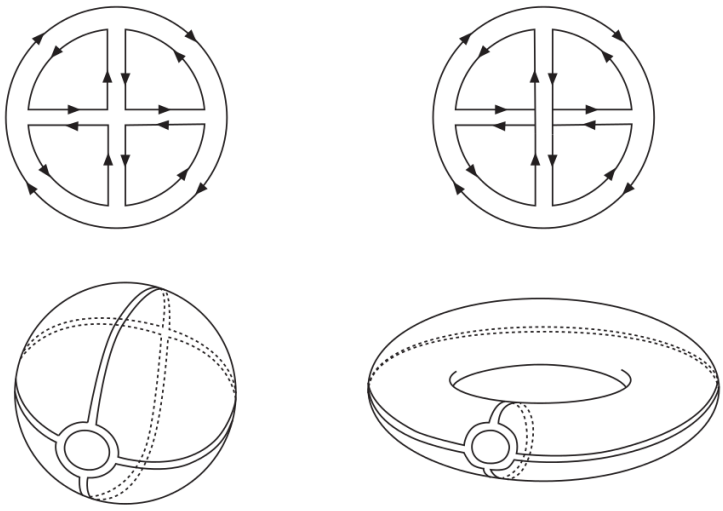

Figure 2.2: Four loop vacuum diagrams and the Riemann surfaces associated to each one. The left side contribution has $h = 0$ handles and thus can be arranged in the surface of a 2-sphere. The right one has $h = 1$ handles and is represented as a torus.

For the sake of completeness, it is worth commenting that, in the examples above, one can check that the left side diagram is composed of five color loops, one four-vertex and four three-vertices so the factor associated is $r = N^5 g^{2+4} = N^2 \lambda_t^3$, the Euler characteristic is $\chi = 2 - 2h = 2$ and, indeed, $h = 0$. Similarly, the right side one is associated with two loops and four three-vertices so $r = N^2 g^4 = \lambda_t^2 N^0$, therefore $\chi = 0$ and $h = 1$.

2.2 Regge Trajectories in 1+1 dimensions

This section is dedicated to the study of the agreement between the theoretical formulation of QCD in the 't Hooft large-N limit and the phenomeno-

logically formulated Regge trajectories. The latter emerge from the relation between the total spin, J, and the mass, M, of boundary states (mesons and baryons). The relation is linear with respect to M^2:

$$J = \alpha_0 + \alpha_1 M^2 \tag{2.1}$$

This relation can be shown explicitly in 1+1 dimensions and has been proved [7] only recently for $d = 3 + 1$. The large-N limit of QCD shows an analogy with the string model, involving Regge trajectories, which could serve as a hint that a duality between QCD field theory and an underlying string theory could exist. A first approach to this analogy was given by Nambu and is addressed in [4]. Here it is shown that a string of length $2a$ and tension σ, binding a massless, spinless quark-antiquark pair, has a maximum angular momentum $J = \sigma\pi a^2/2$ and a total mass $M = \sigma\pi a$. Comparing these results we find the relation

$$M^2 = 2\pi\sigma J$$

which is indeed a straight Regge trajectory, with $\alpha_0 = 0$.

2.2.1 Feynman rules in light cone notation

Once the large-N limit has been introduced, we can begin our first analysis focusing on the variation of space-time dimensions. Following 't Hooft's paper [8], we will show that QCD is compatible with Regge trajectories.

The Lagrangian for QCD with one fermion flavor in $d = 1 + 1$ is

$$\mathcal{L} = \overline{\psi}(i\not{D} - m)\psi - \frac{1}{4}(F^a_{\mu\nu})^2 \tag{2.2}$$

where

$$D_\mu = \partial_\mu - igA^a_\mu t^a \qquad F^a_{\mu\nu} = \partial_{[\mu}A^a_{\nu]} + gf^{abc}A^b_\mu A^c_\nu \tag{2.3}$$

and the Lorentz indices μ, ν only take the values 0 and 1. Calculations can be further simplified if we make use of light cone coordinates [4]:

$$x^\pm = \frac{1}{\sqrt{2}}(x^1 \pm x^0) \qquad p_\pm = \frac{1}{\sqrt{2}}(p_1 \pm p_0) \tag{2.4}$$

In this notation, the metric follows from $x_\mu p^\mu = x_+p^+ + x_-p^- = x_+p_- + x_-p_+$. Then $g_{+-} = g_{-+} = 1/2$. In 1+1 dimensions, the light cone gauge condition $A_+ = 0$ also implies [9] $A_- = 0$ and thus $F_{+-} = -\partial_- A_+$. This implies that, since the three-point vertex arises from the crossed term in

[4] For a more general treatment of 3+1 dimensional QCD in light cone coordinates see [9].

$(F^a_{\mu\nu})^2$ and the four-point vertex from the square of $gf^{abc}A^b_\mu A^c_\nu$, they will not appear in this gauge.

The algebra for the Dirac gamma matrices is simply $\gamma_-^2 = \gamma_+^2 = 0$ and $\{\gamma_-, \gamma_+\} = 2$. The former relation simplifies the Feynman rules as figure 2.3 shows: given that the only vertex contains γ_-, the only term which can survive in the quark propagator is the one proportional to γ_+. Therefore we can simply remove the matrices as in the right side of the figure.

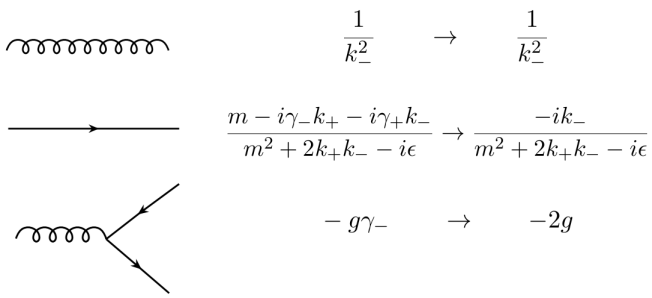

Figure 2.3: Feynman rules in 1+1 dimensions using light cone coordinates

2.2.2 Renormalization

The renormalization of this theory is simple in the large-N limit. We only deal with planar diagrams, as the ones described in section 2.1, in which the gauge field lines do not cross each other and only connect with fermion lines. Then, we have ladder diagrams which fulfill a bootstrap equation for the 1-particle irreducible self-energy amplitude (1PI), $i\Gamma(k)$. Figure 2.4 shows the diagrammatic representation of this bootstrap equation.

$$i\Gamma(p) = \frac{4g^2}{(2\pi)^2 i} \int \mathrm{d}k_+ \mathrm{d}k_- \frac{-i(k_- + p_-)}{k_-^2(m^2 + [2(k_+ + p_+) - \Gamma(k+p)](k_- + p_-) - i\epsilon)} \tag{2.5}$$

From equation (2.5) we see that a simple shift $k_+ + p_+ \rightarrow k_+$ does not affect the result of the integral so $i\Gamma$ cannot depend on p_+.

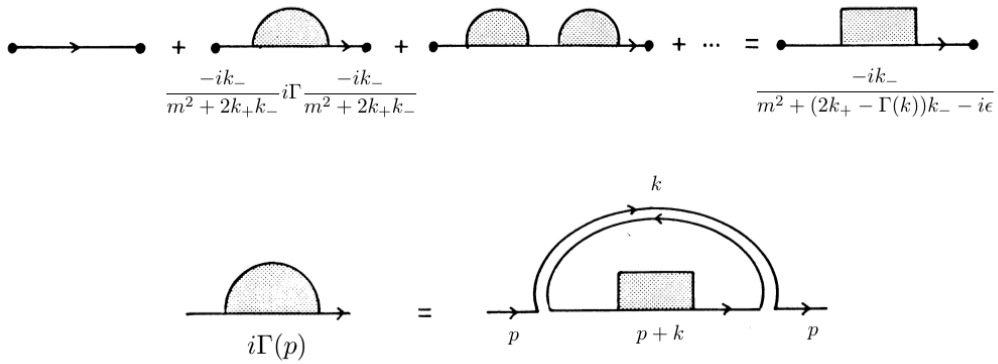

Figure 2.4: Renormalization of the planar, 1+1 dimensional quark self-energy. Top: Definitions of the 1-particle irreducible amplitude $i\Gamma(k)$ and the dressed propagator in the right hand side. Bottom: bootstrap equation satisfied by the amplitudes above. Figures adapted from [8].

After the computation, which we will not perform, we obtain the simple result for the 1PI, in terms of an infrared cutoff Λ_{IR} (the final result of this discussion does not depend on such cutoff):

$$i\Gamma(p_-) = -\frac{ig^2}{\pi}\left(\frac{\text{sign}(p_-)}{\Lambda_{IR}} - \frac{1}{p_-}\right) \tag{2.6}$$

And the dressed (or complete) propagator becomes, in terms of a shifted mass $M^2 = m^2 + g^2/\pi$,

$$S_c(k) = \frac{-ik_-}{m^2+(2k_+-\Gamma(k_-))k_- - i\epsilon} = \frac{-ik_-}{M^2+2k_+k_- + \frac{g^2|k_-|}{\pi\Lambda_{IR}} - i\epsilon} \tag{2.7}$$

Notice that the infrared divergence of this propagator shows that there cannot be free quark states, as confinement requires. Moreover, the following discussion proves that bound states of a quark-antiquark pair (mesons) are allowed and have definite masses.

2.2.3 Two particle states

With the result for the dressed propagator we can make a first approach to the spectrum of two-particle states, which is governed by the homogeneous Bethe-Salpeter equation in momentum space [10]:

$$\Psi(p_1,p_2) = S_c(p_1)S_c(p_2)\int \mathrm{d}^4p_1'\mathrm{d}^4p_2' K(p_1,p_2;p_1',p_2')\Psi(p_1',p_2') \tag{2.8}$$

Here $\Psi(p_1, p_2)$ is the wave function for a two-particle state in momentum space and $K(p_1, p_2; p_1', p_2')$ is the irreducible interaction kernel, which takes the form of a one-gluon exchange in the planar approximation. This interaction is shown in figure 2.5.

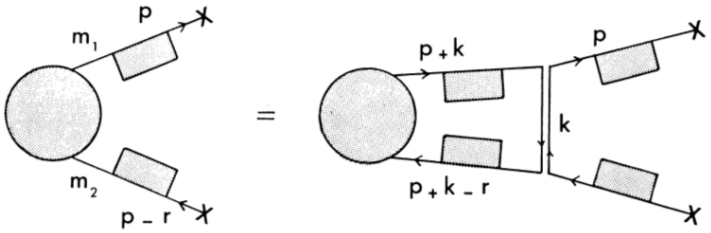

Figure 2.5: Two particle interaction via gluon exchange.

Thus, equation (2.8) takes the form

$$\Psi(p, r) = \frac{4g^2}{(2\pi)^2 i} S_c(p_-) S_c(p_- - r_-) \iint \frac{1}{k_-^2} \Psi(p + k, r)\ \mathrm{d}k_+ \mathrm{d}k_- \tag{2.9}$$

This equation can be brought to the non-analytic form (2.10), which removes the dependence on the cutoff frequency, Λ_{IR}, and allows us to study the spectrum.

$$\mu^2 \Phi(x) = \left(\frac{a_1}{x} + \frac{a_2}{1-x} \right) \Phi(x) - \mathcal{P} \int_0^1 \frac{\Phi(y)}{(y-x)^2} \mathrm{d}y \tag{2.10}$$

where μ^2 is the squared mass of the boundary state in units of g^2/π

$$x = \frac{p_-}{r_-} \qquad \mu^2 = -2\frac{\pi}{g^2} r_+ r_-$$

$$a_{1,2} = \frac{\pi}{g^2} M_{1,2}^2 \qquad \Phi(x) = \int \Psi(p_+, x) \mathrm{d}p_+$$

and $\mathcal{P}$ denotes the principal value integral [5]

Equation (2.10) can be interpreted as a Hamiltonian acting on $\Psi(x)$ with a diagonal term (the first one on the r.h.s.) and an off-diagonal term which couples the states $\Psi(x)$ and $\Psi(y)$ via integration, as explained in [3]. The poles in the original propagators determine the boundary conditions as $\Psi(0) = \Psi(1) = 0$, so the eigenstates $\Psi(x)$ must be periodic and we can use the ansatz $\Psi(x) = e^{i\omega x}$. Now, if we approximate $a_{1,2} \approx 0$ and extend the limits of the integration to infinity we get:

$$\mathcal{P} \int_0^1 \frac{e^{i\omega y}}{(y-x)^2} \mathrm{d}y \approx \mathcal{P} \int_{-\infty}^{\infty} \frac{e^{i\omega y}}{(y-x)^2} \mathrm{d}y = -\pi |\omega| e^{i\omega x} \tag{2.11}$$

[5] $\mathcal{P} \int \frac{\Psi(y)}{y^2} \mathrm{d}y = \frac{1}{2} \int \frac{\Psi(y+i\epsilon)}{(y+i\epsilon)^2} \mathrm{d}y + \frac{1}{2} \int \frac{\Psi(y-i\epsilon)}{(y-i\epsilon)^2} \mathrm{d}y$

So, applying the boundary conditions, we get the relation $\omega = k\pi$ and the eigenstates can be approximated as $\Psi(x)_k \approx \sin(k\pi x)$, $(k = 1, 2...)$ with eigenvalues

$$\mu_k^2 \approx \pi^2 k \tag{2.12}$$

which is of the same form as (2.1), with the quantized angular momentum, J, proportional to $k = 1, 2....$ So the Regge-trajectory phenomenology is recovered in 1+1 dimensions. Deviations from the straight line (for $\alpha_0 = 0$) are expected to arise from a higher order approximation where a non-zero value of $a_{1,2}$ and the finiteness of the integration in (2.11) contribute to α_0.

However, the simplification of this problem by reducing to two the number of dimensions leads to lack of transverse motion and thus of the notion of angular momentum and spin, so the total momentum J in (2.1) could only refer to a principal quantum number k. Moreover, the $1/N$ expansion in two dimensions does not have baryons (which are also colorless) in the spectrum, which are also colorless, so the model cannot provide a complete proof of confinement.

2.3 Higher dimensional QCD and the ϵ-expansion

In this section we will study some properties of QCD in higher dimensions, $1 + 1 < d < 3 + 1$, using the beta function of the gauge coupling in the ϵ-expansion. In section 3 we compare these results to the corresponding ones in QED, while in section 4 we explore different limits in Nf and N of the QCD beta function for a fixed spacetime dimension.

When two spatial dimensions are considered, angular momentum appears in the normal direction, so we cannot expect the same results as in $d = 1 + 1$. Moreover, exactly solvable models are hard to find and perturbation theory in the coupling is often required. Here we show that, as far as the beta function is concerned, the effect of decreasing dimensionality, from $d = 3+1$, does not bring up non-trivial fixed points in the large-N limit and, thus, the theories do not qualitatively differ from the physical scenario with $d = 3+1$. Nevertheless, beyond the large-N limit, and with varying flavor content Nf, different fixed point structures appear. This will be analysed in section 4.

To perform this analysis we will make use of the ϵ-expansion according to the minimal substraction (MS) renormalization scheme. A brief argument is given here to justify the term involving ϵ in the beta function that we will study. For a more exhaustive treatment of the ϵ-expansion in the MS scheme we refer to [11].

The following argument can be found in Peskin & Schroeder [12]. Consider a Lagrangian in d dimensions with a mass term and a self-interaction $\lambda\phi^4$. The

coupling constant λ is dimensionless only in 4 dimensions. We redefine it to remain so in d dimensions by introducing a scale μ. With this substitution the Lagrangian is written as:

$$\mathcal{L} = \mathcal{L}_0 - \frac{1}{4}\lambda\mu^{4-d}\phi^4 \tag{2.13}$$

where $\mathcal{L}_0$ is the Lagrangian for the free scalar renormalized at the scale μ[6]. Then the beta function is shifted by the contribution of the mass dimension of λ:

$$\beta = \mu\frac{\partial\lambda}{\partial\mu} = -\epsilon\lambda + \beta^{(4)}(\lambda) \tag{2.14}$$

where $d = 4 - \epsilon$ and $\beta^{(4)}(\lambda)$ refers to the ordinary four-dimensional beta function. This is the source for Wilson-Fisher-like fixed points. We will apply this recipe first to QCD in the large-N limit, and then we will comment on the cases with finite N and N_f. The beta function for QCD has been computed to four-loop order [13] but in this approach we will keep it to the leading (one-loop) order with fermions in the fundamental SU(N) representation:

$$\beta(g) = \mu\frac{\partial g}{\partial\mu} = -\frac{\epsilon}{2}g - \frac{g^3}{(4\pi)^2}\left(\frac{11}{3}N - \frac{2}{3}N_f\right). \tag{2.15}$$

This result is also in agreement with Gracey in [14], who also uses the ϵ expansion to study the beta function in the large-N_f limit. We now implement the large N limit and rewrite the beta function in terms of the 't Hooft parameter $\lambda_t = g^2N$:

$$\beta(\lambda_t) = \mu\frac{\partial\lambda_t}{\partial\mu} = -\epsilon\lambda_t - 2\frac{\lambda_t^2}{(4\pi)^2}\left(\frac{11}{3} - \frac{2N_f}{3N}\right), \tag{2.16}$$

where the last term in the parenthesis disappears when we take $N \to \infty$. So, in this limit a non-trivial solution for λ_t exists but does not fulfill the defining condition of being a positive quantity. Thus, we conclude that there is no Wilson-Fisher-like IRFP in the large-N limit of QCD and the fixed-point structure of the theory does not differ from the 4 dimensional case, $\epsilon = 0$. The same result holds when considering higher-order terms in g or λ_t: keeping only the coefficients multiplying the highest power of N in each term of the $\beta(g)$ loop expansion, we only get negative or complex solutions λ_t^* (the possible fixed point), which are not physical[7].

[6] Peskin and Schroeder also regard here a mass term, $-\frac{1}{2}\rho_m\mu^2\phi_\mu^2$, but it is not of interest in the current discussion

[7] For example, to three-loop order, the equation to solve for λ_t^* is

$$\frac{\epsilon}{2} + \frac{11}{3}\frac{\lambda_t^*}{(4\pi)^2} + \frac{34}{3}\frac{(\lambda_t^*)^2}{(4\pi)^4} + \frac{2857}{54}\frac{(\lambda_t^*)^3}{(4\pi)^6} = 0.$$

Since all coefficients are positive the solution for λ_t^* cannot be positive too.

3 Comparison with QED

We find instructive to compare the obtained results for the SU(N) gauge theory with the U(1) case also in varying dimensions. That is, on one side, confinement and Regge-like spectrum appear when considering 1+1 dimensions and, on the other side, the fact that no IRFP exist when dealing with higher dimensions, $d = 4 - \epsilon$, at least when dealing with the large-N limit.

In the first place, we remark that confinement arises in 2-dimensional QED (QED_2) too. The fundamental difference is the spectrum of this theory, which consist merely of a massive particle with the quantum numbers of the photon [15]. Thus, by taking the limit $N = 1$ in QCD we do not recover the result from QED. This is no contradiction since the planar limit, on which we have relied to obtain the spectrum for QCD_2, does not provide a good approximation when we set $N = 1$.

The striking similarity involving confinement in QED_2 is addressed in [16]. In this paper, the authors solve the two-point Green's function for a massless fermion in the Coulomb gauge ($A_1 = 0$) and in terms of a scalar field ϕ. The result[8] involves an exponential which tends to zero at $x_0 = 0$ and $x_1 \to 0$ (so the Green function reduces to the free case) but diverges for $x_0 \neq 0, \forall x_1$ and the propagator vanishes. This is physically explained by the non-vanishing electric field at large distances which appears in two spacetime dimensions. Hence, the probability for the vacuum polarization to appear is proportional to the spatial volume and, at any time after inserting a fermion, pairs are created and the probability to find only one fermion again (given by the 2-point function) is null.

On the other hand, the ϵ-expansion does reveal a Wilson-Fisher IRFP in QED. This result obtained in [1] in a similar fashion to that sketched above. In this article, the two-point function of a general operator is considered in the limit $\epsilon << 1$ and $p \to 0$ (IR limit):

$$\langle \mathcal{O}(p)\mathcal{O}(-p)\rangle \approx p^{2\Delta-d} p^{2\gamma_1 c\epsilon/\beta_1} + O(\epsilon^2) \tag{3.1}$$

in terms of Δ, the operator dimension in $d = 4$, $c\epsilon$, the mass dimension of the coupling constant in $d = 4 - 2\epsilon$, with c some integer number, and the leading-order coefficients for the beta and gamma functions:

[8] The exact result computed was $\langle 0|\, \psi^\dagger(x)\psi(0)\, |0\rangle = \langle 0|\, \chi^\dagger(x)\chi(0)\, |0\rangle\, e^{K(x)}$, where $\chi(x)$ is the free field satisfying Dirac equation and

$$K(x) \propto \int \mathrm{d}k \frac{(\omega_k - k)^2}{k^2\omega}(e^{i(kx_1 - \omega x_0)} - 1)$$

$$\beta(g) = \beta_1 g^2 + O(g^3) \qquad \gamma(g) = \gamma_1 g + O(g^2)$$

The ϵ term in equation (3.1) contributes as a shift in the IR dimension of the operator $\mathcal{O}$, $\Delta_{IR} - \Delta = \gamma_1 c\epsilon/\beta_1$, which corresponds to the value of the anomalous dimension, γ, evaluated at the fixed point: as in section 2.3, the beta function for the dimensionless parameter $\lambda = g\mu^{-c\epsilon}$, has a non-trivial zero at λ_*,

$$\beta(\lambda_*) = 0 = -c\epsilon\lambda_* + \beta_1\lambda_*^2 + O(\lambda_*^3) \implies \lambda_* = \frac{c\epsilon}{\beta_1}$$

The authors then evaluate the IR dimensions of different currents in QED (such as $J^s_\mu = \sum_i \overline{\psi}_i \gamma_\mu \gamma_5 \psi^i$) but this is out of the scope of the present paper. Nevertheless, in order to do so, the Wilson-Fisher fixed point for QED is calculated in the article in terms of $\hat{e} = e\mu^{-\epsilon}$:

$$(\hat{e}_*) = 0 = -\epsilon\hat{e}_* + \frac{N_f}{12\pi^2}\hat{e}_*^3 + O(\hat{e}_*^5) \implies \hat{e}_*^2 = \frac{12\pi^2\epsilon}{N_f} \tag{3.2}$$

Thus, we see that, contrary to QCD, QED does develop a non-trivial IRFP for $d < 3 + 1$ and the coupling constant is proportional to ϵ itself. It is also interesting to notice the effect of screening in the inverse proportionality with the number of fermion flavors N_f. The more virtual fermions participating in the vacuum fluctuation, the more difficult to escape from the IR freedom regime and develop a non-trivial IRFP, so $\hat{e}_*^2$ becomes smaller. On the other hand, the screening effect would diminish if we restricted to lower dimensions; intuitively, less virtual fermions can surround the source of $\hat{e}$ in the area of a circle than in the volume of a sphere.

4 The QCD beta function in the large-N_f limit

We will now move towards a different limit situation by studying how the beta function shape changes by increasing the number of fermion flavors present in the theory and keeping the number of colors N fixed.

4.1 UV-free, IR-free theories and non-trivial fixed points

In the context of the renormalization group, there exist three possible behaviors of the beta function, in a small region of the corresponding coupling constant, λ: it can be positive, negative or exactly zero.

A positive beta function appears for the so-called infrared-free theories, with regular (4-dimensional) QED as a paradigm. For this case, at one-loop order, we have

$$\beta(e) = \frac{N_f e^3}{12\pi^2} \tag{4.1}$$

The running coupling constant, $\bar{e}$, satisfies the renormalization group equation:

$$\frac{\mathrm{d}}{\mathrm{d}\log(p/\mu)}\bar{e}(p,e) = \beta(\bar{e}), \qquad \bar{e}(\mu,e) = e \tag{4.2}$$

in terms of the momentum p and the renormalization scale μ. By integrating and simplifying we get the relation for the evolution of the running coupling constant:

$$\bar{e}^2(p) = \frac{e^2}{1 - (N_f e^2/6\pi^2)\log(p/\mu)} \tag{4.3}$$

From equation (4.3) we see that the running coupling constant flows to zero in the infrared ($p \to 0$), in other words the coupling becomes small at large distances and perturbation theory provides accurate predictions in this regime. Hence the name "infrared-free theories". Nevertheless, in the ultraviolet limit, QED develops a Landau pole: $\bar{e}(p)$ becomes large at small but finite distances and Feynman diagram perturbation theory is no longer applicable. The running coupling constant diverges (has a pole) at $\mu = p\exp(6\pi^2/\bar{e}^2)$. The beta function of a QED-like theory, IR-free and with a Landau pole in the UV limit, has the form of figure 4.1. In the figure we used the notation $\alpha = e^2/4\pi$ and the values $N = 1$ (to recover U(1) gauge symmetry) and $N_f = 6$, as indicated, from a more general computation discussed below.

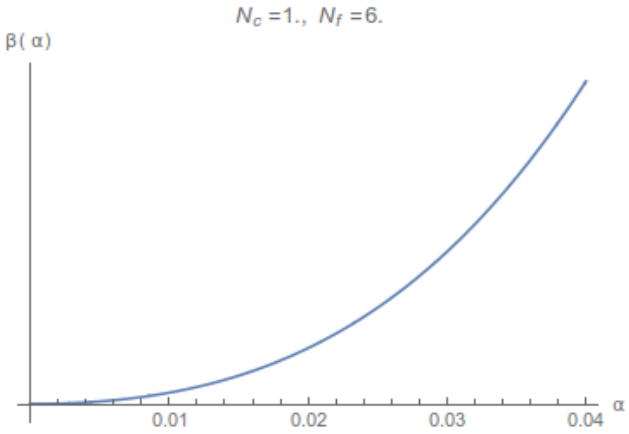

Figure 4.1: Positive beta function with no non-trivial fixed points.

If the coefficient appearing in the beta function is negative we encounter the case of asymptotic freedom, as seen for QED in $d = 1+1$ and large-N QCD.

For the latter example, the beta function in $d = 3 + 1$ can be written as in equation (2.16) ($\epsilon = 0$):

$$\beta(\lambda_t) = -\frac{22}{3}\frac{\lambda_t^2}{(4\pi)^2} \equiv -\beta_0 \lambda_t^2 \tag{4.4}$$

using 't Hooft's parameter $\lambda_t = g^2 N$. The evolution of the running coupling constant, similarly to equation (4.3), now obeys the relation

$$\overline{\lambda_t}(p) = \frac{\lambda_t}{1 + \beta_0 \lambda_t \log(p/\mu)} \tag{4.5}$$

The positive coefficient in front of $\log(p/\mu)$ implies it tends to zero in the ultraviolet limit ($p \to \infty$) and Feynman diagrams perturbation theory is applicable at short-distance scale. Figure 4.2 shows the behavior of the negative beta function for QCD to three-loop order. Again, we have used the notation $\lambda_t = g^2 N$ and we have neglected the terms in the beta function coefficients containing N in the denominator since $N \to \infty$.

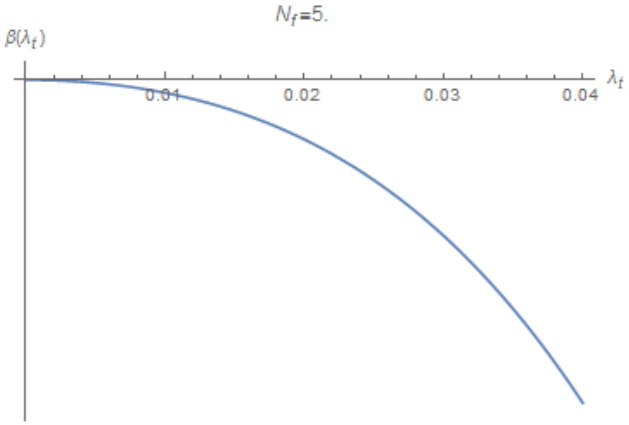

Figure 4.2: Negative beta function with no non-trivial fixed points.

Finally, we now consider the possibility of non-trivial fixed points, by looking for zeros of the beta-function at nonzero coupling. At a fixed point the theory is scale invariant, and in most known examples it is also conformally invariant. We can again distinguish between IR and UV fixed points. The case of a non-trivial UV fixed point, asymptotic safety, will be further discussed in section 5. Both examples of fixed points are depicted in figure 4.3.

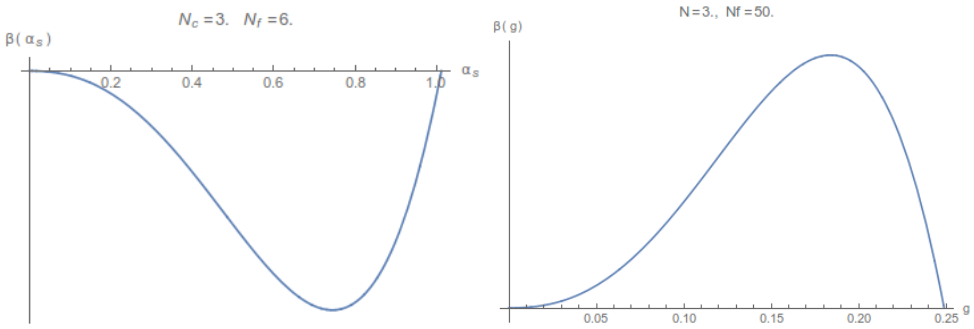

(a) Non-trivial infrared fixed point. (b) Non-trivial ultraviolet fixed point.

Figure 4.3: Possible zeros of the beta function for $(\text{QCD})_4$ at four-loop order.

4.2 Analysis of the beta function derivative

Once we have reviewed the possible phenomena of the theories depending on the values of the beta function, we can analyze how to expect each kind of behavior by simply looking at its derivative. The algorithm to look for stable non-trivial fixed points in the beta function is clear. One simply seeks the zeros of the function, g_0 such that:

$$\beta(g_0) = 0 \tag{4.6}$$

and analyzes whether the function is increasing or decreasing at those points by computing the sign of the derivative: $\frac{\partial\beta(g)}{\partial g}\Big|_{g_0}$. If the derivative is negative, the beta function decreases, as in figure 4.3b, thus we will have found an ultraviolet fixed point. Similarly, if at g_0 the beta function is increasing (positive derivative), then this zero of the beta function will represent an infrared fixed point, as in figure 4.3a. Finally, if equation (4.6) has no real and positive (since we define the coupling constant to be so) solution, then it logically has no fixed points and we encounter the cases of infrared freedom and asymptotic freedom.

As an example we will consider the QCD beta function at three-loop [13] order as a function of $a = \alpha_s/4\pi = g^2/16\pi^2$, with fermions in the fundamental representation and using the MS-scheme:

$$\beta(a, N, N_f) = -\beta_0 a^2 - \beta_1 a^3 - \beta_2 a^4 + O(a^5) \tag{4.7}$$

where

$$\beta_0 = \frac{11}{3}N - \frac{4}{3}N_f$$

$$\beta_1 = \frac{34N^2}{3} - \frac{(N^2-1)\,N_f}{N} - \frac{10NN_f}{3}$$

$$\beta_2 = \frac{2857N^3}{54} + \frac{11\left(N^2-1\right)N_f^2}{18N} - \frac{205}{36}\left(N^2-1\right)N_f + \\ + \frac{\left(N^2-1\right)^2 N_f}{4N^2} + \frac{79NN_f^2}{54} - \frac{1415N^2N_f}{54}$$

Now, applying equation (4.6), we find a pair non-trivial zeroes, a cumbersome expression depending on N and N_f (they differ only by the characteristic $\pm$ sign from a regular second-order equation solution). Their analytic expressions do not provide great insight, so we will not write them and simply call them $a_0^{\pm}$.

Finally, let us study the sign of the beta function derivative evaluated at $a_0^{\pm}$. The value obviously depends on N and N_f, so we will fix one of these parameters, say $N = 5$, and plot $\frac{\partial\beta(a)}{\partial a}\Big|_{a_0^{\pm}}$ as a function of N_f, as shown in figure 4.4.

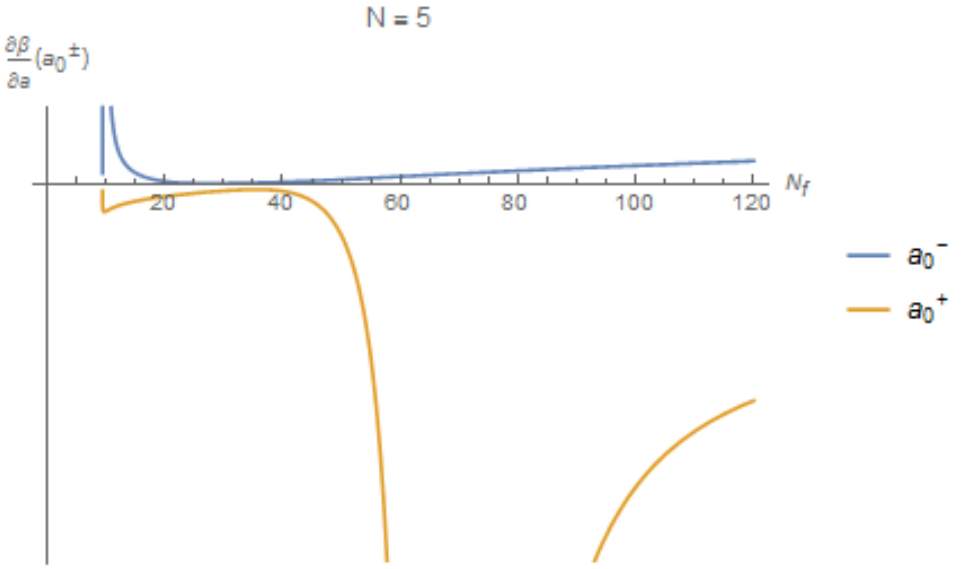

Figure 4.4: Derivative of $\beta(a)$ evaluated at $a_0^{\pm}$ for 5 charge colors. Each line represents one of the two non-trivial solutions of equation (4.6)

In the figure we see that the function is not evaluated at the approximate interval $N_f \in [0, 9.4]$ since here $a_0^{\pm} \notin \mathbb{R}$. Then the function only increases with a. The same holds for $N_f \in [9.4, 9.6]$ (that is, close to the asymptote of the blue line), since here $a_0^{\pm} < 0$. From this asymptote and till the value $N_f \approx 27.5$, (where the blue line reaches the abscissa axis), one of the zeros is real and positive (a_0^-) and the derivative is positive evaluated so we deal with an IRFP. In the interval $N_f \in [27.5, 67]$, i.e. approaching the yellow asymptote from the left, both solutions are again negative, $a_0^{\pm} < 0$, and we now recover the abelian case of IR freedom. Lastly, past the yellow

assymptote, $N_f > 67$, the other zero of the beta function becomes positive, $a_0^+ > 0$ and, since the corresponding derivative is always negative, the theory displays asymptotic safety and we can find an UVFP. The corresponding plots for $\beta(a)$ are shown in figure 4.5.

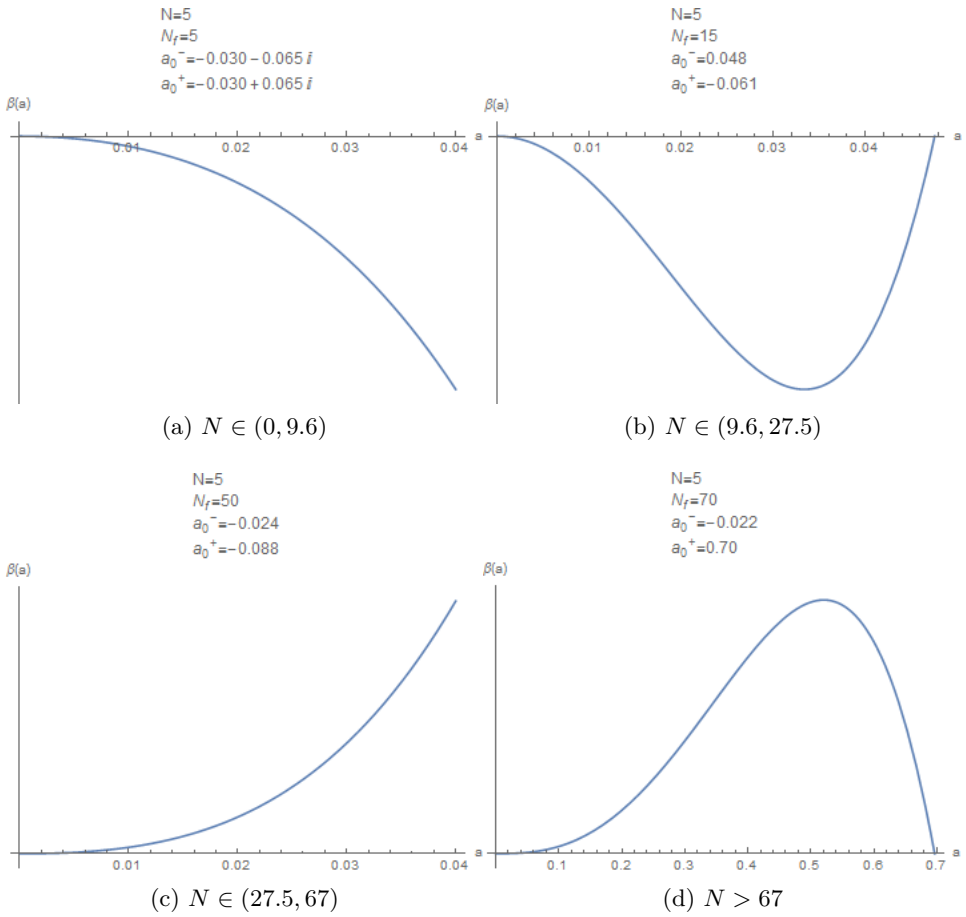

(a) $N \in (0, 9.6)$ (b) $N \in (9.6, 27.5)$

(c) $N \in (27.5, 67)$ (d) $N > 67$

Figure 4.5: Samples of beta functions and its zeroes with varying the number of flavors. $N = 5$ for all the cases. The intervals indicate the approximate range of N_f where this behaviors can be found.

By comparing these results and the analysis performed in the previous section we can notice that by increasing the number of flavors to approach that of colors we arrive at the asymptotic freedom regime, while if the number of flavors is much larger than that of colors the theory is infrared free or develops asymptotic safety. Only for a finite range of both numbers we get the finite theory [9], namely the conformal window. This is physically explained

[9]We call "finite theories" to those with no ultraviolet divergences. Since the coupling constant does not run, it cannot diverge, so the only possible divergences would be asso-

in terms of (anti)screening effects. When the number of color charges is comparable to the number of possible fermions which can appear in pair creation from vacuum fluctuation, the anti-screening effect takes over and confinement is developed in the theory. In the other case screening by pair creation dominates over confinement produced by color and the theory is QED-like (though it might or might not diverge at the Landau pole). This is also reflected in the behavior of the derivative of $\beta(a)$ when varying N. As figure 4.6 shows, if we decrease N, the graph shrinks to lower values of N_f, since we have less colors to compensate the screening and reach the regime where no real positive values of $a_0^{\pm}$ exist, thus where confinement is achieved. Also, for smaller values of N, the interval between the asymptotes disappear as we decrease N_f and we start distinguishing new blue asymptotes and exotic behaviors for $N < 1$. An example of such exotic behavior is depicted in figure 4.7b, where we can see two positive fixed points. This could be ruled out as a non-physical behavior since it only appears for very values of $N \approx 0.1$, so we would barely have gauge symmetry degrees of freedom.

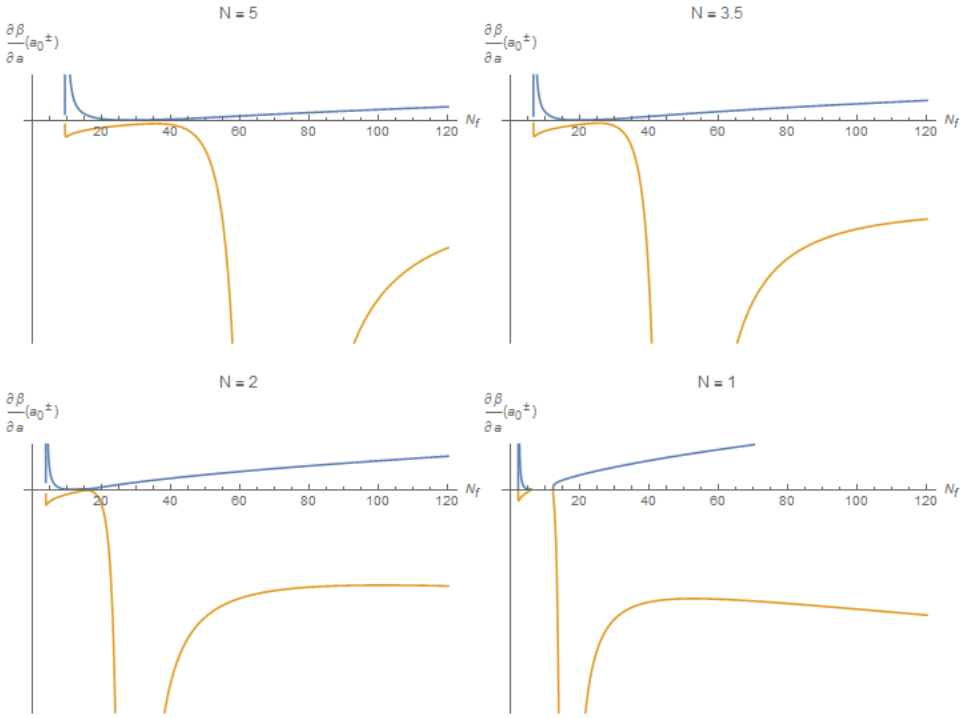

Figure 4.6: Samples of $\frac{\partial \beta(a)}{\partial a}\Big|_{a_0^{\pm}}$ as a function of N_f for different values of N. Shrinking of the values and the disappearance of some intervals can be noticed.

ciated with field rescaling, but they automatically cancel in the computation of S-matrix elements [12].

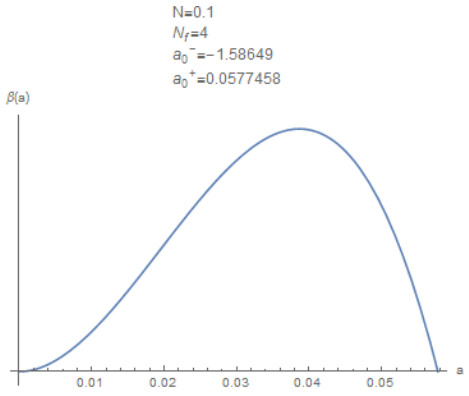

(a) Regular asymptotic safety for $N_f = 4$: only one positive zero

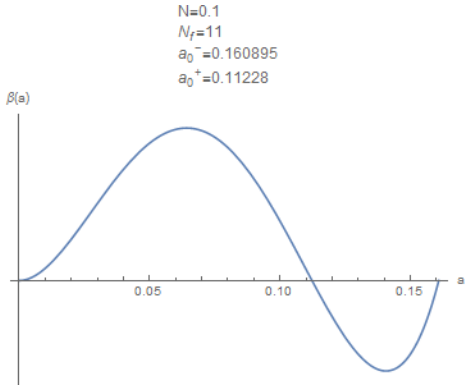

(b) Two zeros in the beta function for $N_f = 11$

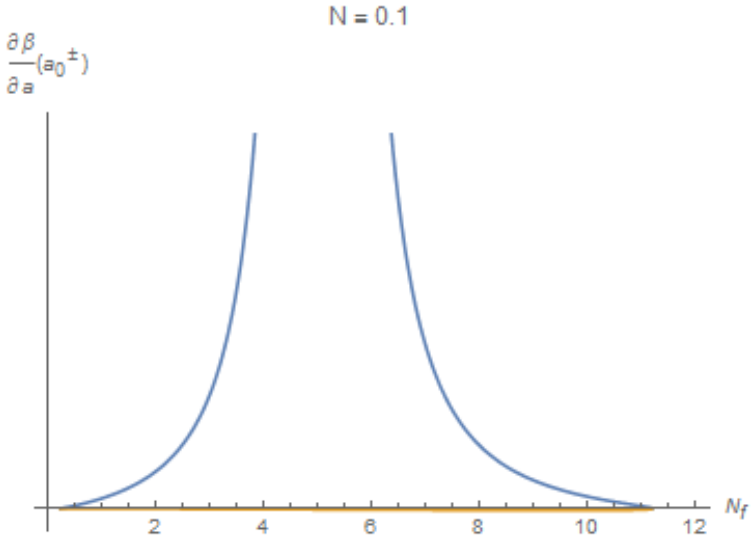

(c) Derivative of β. For $N_f < 5$ only a_0^+ is positive and for $N > 5$ both $a_0^\pm$ are.

Figure 4.7: Exotic behavior of β for $N = 0.1$.

4.3 Checkup of the previous results in the ϵ-expansion

In this section we apply the previous analysis to the theories considered before, namely QCD in the large-N limit and QED. In both cases we will need to introduce a new parameter: ϵ, in order to introduce the dimensional expansion.

It is clear, from the analysis done in figure 4.6, that for a given number of fermion flavors, we can always find a number of colors large enough so that no real positive zeroes of the beta function exist, therefore ultraviolet-free

theories appear in 't Hooft limit. Now we would like to check whether this stands also for different dimensions $d < 3+1$. As we saw in section 2.3, no IR fixed points exist in the large-N limit for any power of g in the ϵ-expansion. Introducing this parameter in our β function we get:

$$\beta(a, N, N_f, \epsilon) = -\epsilon a - \beta_0 a^2 - \beta_1 a^3 - \beta_2 a^4 + O(a^5) \tag{4.8}$$

keeping the same coefficients β_i as above. We follow the same procedure as before only now we will fix $N = 20$, to approach the large-N limit, and we will plot $\frac{\partial\beta(a)}{\partial a}\Big|_{a_0}$ as a function of ϵ for different values of N_f. We have introduced a new power of a in the beta function, hence there will be now three non-trivial zeroes, $a_0^{(i)}$ $(i = 1, 2, 3)$, but only $a_0^{(1)}$ happens to take real values. However, the derivative, evaluated at these points, does take real values but only for N_f large enough, a regime which invalidates the assumption of N being large. We will only show this result for the sake of completeness but we emphasize the fact that it does not represent any previous result.

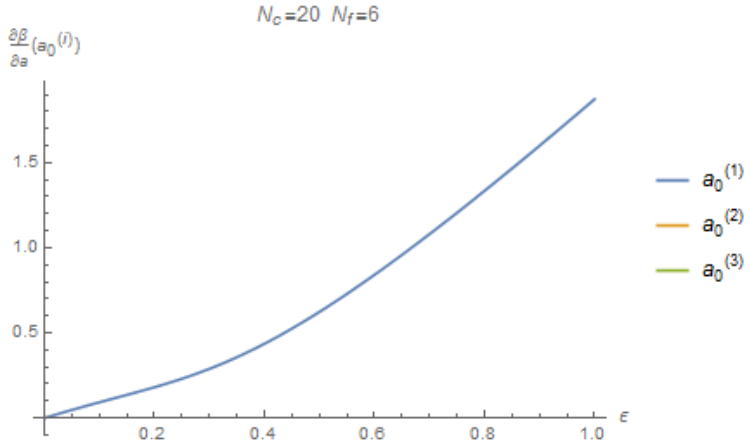

(a) Regular IR freedom for low N_f in any dimension in agreement with the discussion below equation (2.16). $a_m^{(1)} < 0$ in this regime.

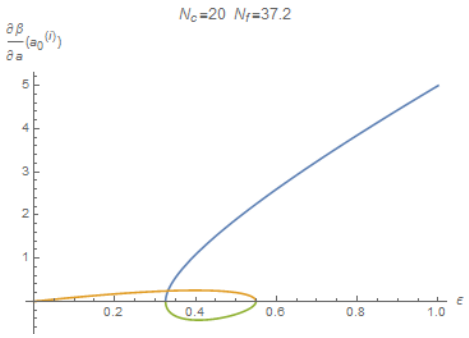

(b) Other lines appear for values of N_f comparable to N.

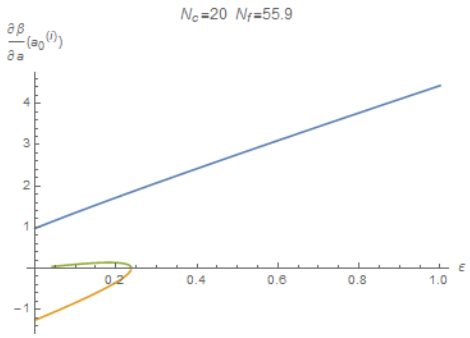

(c) Large-N_f limit. Here $a_0^{(1)}$ is a IRFP since the large-N limit no longer holds.

Figure 4.8: Beta function's derivative for $N = 20$ as a function of the dimensional parameter ϵ. The legend in subfigure 4.8a holds for the others too. Only values of $\epsilon \ll 1$ make sense in the expansion.

Once we have double-checked the result that the ϵ expansion does not bring new fixed points in the large-N limit of QCD, we turn our attention to the abelian U(1) subgroup included in the more general theory, namely QED. To recover this subgroup we need to modify our beta function in agreement with the quadratic Casimir operators [17] for U(1) $C_A = 0, C_F = T_F = 1$. With these values, the coefficients β_0, β_1 of the beta function to two-loop order (for higher order the results are scheme-dependent and it leads to computation problems in the case of QED) are:

$$\beta_0 = \frac{11}{3}C_A - \frac{4}{3}T_F N_f = -\frac{4}{3}N_f$$

$$\beta_1 = \frac{34}{3}C_A^2 - 4C_F T_F N_f - \frac{20}{3}C_A T_F N_f = -4N_f$$

And the beta function, taking into account the ϵ term, is simply:

$$\beta(a) = -\epsilon a + \frac{4}{3} N_f a^2 + 4 N_f a^3 \tag{4.9}$$

The two non-trivial zeroes of the beta function are again of the form $a_0^{\pm}$. Figure 4.9 shows two plots for the derivative with different values of N_f. It shows that increasing the number of fermion flavors does not affect much to the properties of the theory. Figure 4.10 shows the two possible beta functions for $N_f = 1$. As we saw, however small the dimension decrease ϵ is, a IRFP will always appear. Thus, we have extended the result reviewed in section 3 to two-loop order.

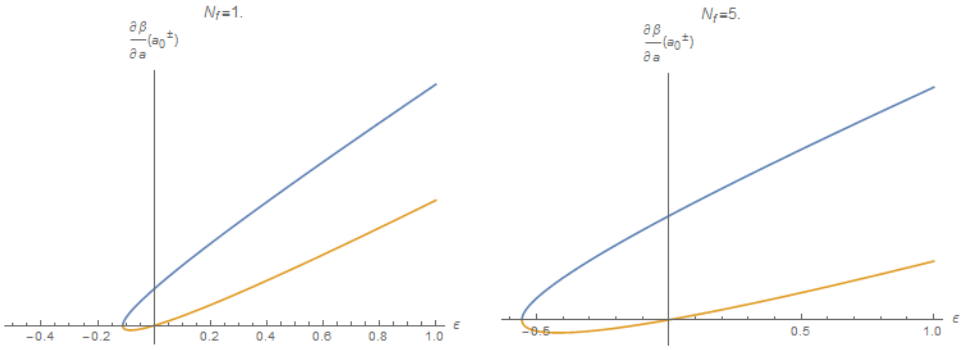

Figure 4.9: Derivative of the QED beta function as a function of ϵ for $N_f = 1, 5$. Only for $\epsilon \neq 0$ does a_m^+ take a different value from 0.

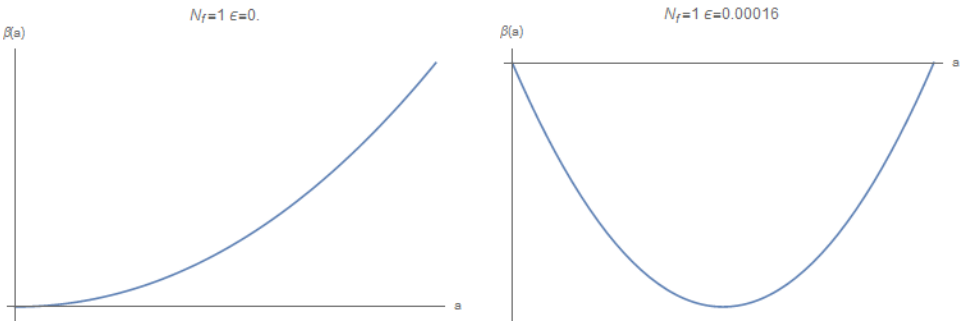

Figure 4.10: Beta function at two-loop order for QED in the ϵ expansion

5 Asymptotic safety in Gauge-Yukawa theories

Now we turn our attention towards a different limit. We have seen that asymptotic freedom always arises in the large-N limit and only for comparable N_f and N do we get non-trivial (i.e. interacting) fixed points. We may

use now a parameter which keeps the ratio N_f/N fixed (since we want them to be comparable) but still small. This is known as the Veneziano limit. We will restrict ourselves to $d = 3 + 1$ and use two couplings as a method to find fixed points.

5.1 Asymptotic safety with one coupling constant

An interacting UV fixed point allows the coupling to follow well-defined Renormalization group trajectories avoiding divergences (such as Landau poles) in the high-energy limit. It is then tempting to think of asymptotic safety as the fundamental theory behind the scalar and the U(1) sector of the standard model, or even to relevant and marginal invariants which dominate the physics in the UV limit, as [2] proposes. We will follow this paper closely in the present section. Another possible application of asymptotic safety would be the simplification of gravity quantisation provided by UV conformal matter [18].

As we have seen in different previous examples, a non-trivial (or non-Gaussian) ultraviolet fixed point appears in theories whose beta functions are of the form

$$\beta(\alpha) = \frac{\mathrm{d}\alpha}{\mathrm{d}\log(p/\mu)} = A\alpha - B\alpha^2 \tag{5.1}$$

for a generic coupling α and two positive numbers A and B. The linear-term coefficient relates to the mass dimension of the coupling $-A$, that is, the ϵ parameter we have used previously. There is obviously a trivial fixed point at $\alpha* = 0$ and a non-trivial one at $\alpha_* = A/B$. For this fixed point to be perturbatively accessible ($\alpha_* \ll 1$), we need either $A \ll 1$, for fixed B, or $B \gg 1$ for fixed A. In the vicinity of α_* one can use (5.1) to expand α and obtain

$$\alpha(p) \approx \alpha_* + C\left(\frac{p}{\mu}\right)^{\vartheta} \tag{5.2}$$

with C an integration constant and ϑ a universal number which arises as the eigenvalue of the stability matrix, which in this case is one-dimensional:

$$\vartheta = \left.\frac{\partial\beta}{\partial\alpha}\right|_{\alpha_*} \tag{5.3}$$

For the r.h.s. of (5.1), this gives $\vartheta = A$ for the Gaussian fixed point and $\vartheta = -A$ for the non-Gaussian one. In the assumption that $A > 0$, the deviation from the fixed point decreases as the momentum $p \to \infty$, so we deal with a UV non-trivial fixed point. Conversely, the Gaussian fixed point is approached as $p \to 0$, therefore it is an IRFP. We emphasize the fact that the eigenvalue ϑ is universal and characterizes the scaling of the coupling in a domain close to the fixed point.

5.2 UV fixed points in Gauge-Yukawa theory

The Lagrangian considered in [2] adds a Yukawa-like interaction to the Yang-Mills Lagrangian (2.1) in the fundamental representation. The relevant terms in this discussion are:

$$\mathcal{L} = -\frac{1}{2}(F^a_{\mu\nu})^2 + i\overline{\psi}\not{D}\psi + y\mathrm{Tr}(\overline{\psi}_L H\psi_R + \overline{\psi}_R H^\dagger \psi_L) \tag{5.4}$$

where the decomposition $\psi_{L/R} = \frac{1}{2}(1 \pm \gamma_5)\psi$ is used, ψ contains N_f massless Dirac fermions in the fundamental representation and H represents a complex $N_f \times N_f$ matrix scalar field. In this paper we will ignore the contributions of the mass, gauge-fixing and ghost terms as well as the higher-order corrections from the scalar kinetic and self-interaction terms arising from the full scalar propagator term $\frac{1}{2}(D_\mu H^i)^2$ and the quartic polynomial $-\frac{1}{4}\lambda_{abcd}H_aH_bH_cH_d$. The explicit expressions for the beta functions are given in terms of the normalized coupling constants

$$a_g = \frac{g^2 N}{(4\pi)^2} \qquad a_y = \frac{y^2 N}{(4\pi)^2}$$

which naturally introduce the parameter

$$n = \frac{N_f}{N} - \frac{11}{2} \tag{5.5}$$

This parameter is controlled by varying the relation N_f/N, which characterizes the Veneziano limit, so that both N_f and N are large but n remains finite and small. In terms of n, the coefficient β_0 in equation (4.7), now becomes simply $\beta_0 = \frac{4}{3}n$, also in agreement with equation (2.1), only now considering strictly 4 spacetime dimensions, so $\epsilon = 0$, and the coefficient in (5.1) becomes $A = 0$. Thus, to one-loop order, the beta function for the gauge sector is $\beta_g = \frac{4n}{3}a_g^2$. This function has a doubly-degenerated Gaussian IR fixed point only if $n > 0$. The other case, $n < 0$, would display ultraviolet freedom. Once higher loop corrections are introduced, there might exist non-trivial fixed points. Then, the condition for it to be a UVFP in the perturbative regime translates into

$$0 \leq n \ll 1 \tag{5.6}$$

When we include two-loop order corrections, the beta function takes the form

$$\beta_g = -\frac{4n}{3}a_g^2 + \left(25 + \frac{26}{3}n\right)a_g^3$$

with a doubly-degenerated Gaussian fixed point and a non-trivial one at

$$a_g^* = -\frac{4n}{75 + 26n}$$

but in the assumption (5.6), $a_g^* < 0$, so the solution is non-physical. So, in principle, it would seem that both in the large-N and the Veneziano limits, no UVFP exist even if we considered $d < 3+1$ dimensions by the ϵ-expansion (the same argument as in section 2.3 holds here)[10]. This motivates the introduction of the Yukawa coupling constant a_y. Given a theory combining both Gauge and Yukawa interaction, the beta functions for both a_g and a_y depend mixedly on both couplings leading to possible new fixed points as we will shortly see. The authors of [2] consider two combinations: first, Gauge and Yukawa interactions at two- and one-loop order, respectively, and second, Gauge, Yukawa and dynamical scalars at three-, two- and one-loop order respectively. We will not include the scalar interaction corrections in this paper. [2] refers to the results of [19–21] for the explicit expressions. In this series of papers, several diagrams are computed for general gauge R_ξ and general representation of the group under which the scalar and spinor fields transform. A sample of such diagrams is shown in figure 5.1.

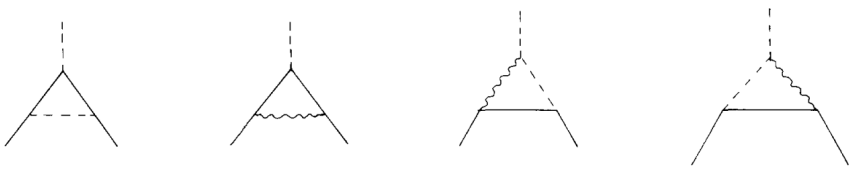

Figure 5.1: One-loop correction to the proper Yukawa vertex. Usual notation is understood: fermions are represented by solid lines, gauge bosons by wavy lines and scalar mesons by dashed lines. Courtesy of [20].

The two considered beta functions are, then:

$$\beta_g = a_g^2 \left\{ \frac{4}{3}n + \left(25 + \frac{26}{3}n\right) a_g - \left(\frac{11}{2} + n\right)^2 a_y \right\} \tag{5.7a}$$

$$\beta_y = a_y\{(13 + 2n)a_y - 6a_g\} \tag{5.7b}$$

The coupled system displays a Gaussian fixed point at $(a_g^*, a_y^*) = (0, 0)$, a non-physical interacting fixed point at $(a_g^*, a_y^*) = (-\frac{4n}{75+26n}, 0)$ —as noted already—, and a new non-trivial, UVFP at

$$a_g^* = \frac{26n + n^2}{57 - 46n - 8n^2} = \frac{26}{57}n + \frac{1424}{3249}n^2 + O(n^3) \tag{5.8a}$$

$$a_y^* = \frac{12n}{57 - 46n - 8n} = \frac{4}{19}n + \frac{184}{1083}n^2 + O(n^3) \tag{5.8b}$$

[10]However, we would like to emphasize that the UV fixed points can be found in the three- and four-loop beta functions if we do not impose the large-N limit restriction or the condition (5.6), as we did in section 4.2.

which accomplishes $(a_g^*, a_y^*) > (0, 0)$, so it is physically relevant. This UVFP can be used to linearize the beta functions, insofar as its behavior can be approximated, in a close domain, as

$$\beta_i \approx \sum_j M_{ij}(a_j - a_j^*) \tag{5.9}$$

where $i = (g, y)$ and $M_{ij} = \frac{\partial \beta_i}{\partial \alpha_j}\Big|_*$ is the 2×2 stability matrix whose eigenvalues can be analytically found:

$$\vartheta_1 = -\frac{104}{171}n^2 + \frac{2296}{3249}n^3 - \frac{1387768}{1666737}n^4 + O(n^5) \tag{5.10a}$$

$$\vartheta_2 = \frac{52}{19}n + \frac{9140}{1083}n^2 + \frac{2518432}{185193}n^4 + O(n^4) \tag{5.10b}$$

Since $\vartheta_1 < 0$ and $\vartheta_2 > 0$, for n fulfilling (5.6), the gauge-Yukawa system develops, respectively, a relevant and an irrelevant eigendirection. Being the dependence on n at leading order $\vartheta_1 \sim n^2$ and $\vartheta_2 \sim n$, (5.6) also implies ϑ_2 is parametrically larger.

Since at the UVFP an irrelevant (decreasing) and a relevant (growing) direction are developed, the short distance behavior in that point can be described by a lower-dimensional UV critical surface. To do so we will express one of the couplings in terms of the other, for example $a_y = F(a_g)$. This close domain is well approximated by the linearization of the couplings. Similarly to the integration performed to obtain (5.2), we generalize the result for the case of two couplings:

$$a_g(p) \approx a_y^* + \sum_k c_k V_g^k \left(\frac{p}{\mu}\right)^{\vartheta_k} \tag{5.11a}$$

$$a_y(p) \approx a_g^* + \sum_k c_k V_y^k \left(\frac{p}{\mu}\right)^{\vartheta_k} \tag{5.11b}$$

where V_g^k, V_y^k are the eigenvectors corresponding to the eigenvalues ϑ_k and c_k are free parameters. Now, since (a_g^*, a_y^*) is a UVFP, we need $(a_g(p), a_y(p))$ to approach it at $p \to \infty$. However, we have seen that $\vartheta_1 < 0 < \vartheta_2$, so this is only accomplished if we set $c_2 = 0$, which leaves c_1 undetermined insofar as we can use it to express one coupling in terms of the other:

$$a_y = F(a_g) = \left(\frac{6}{13} - \frac{88}{507}n\right) a_g + \frac{8}{171}n^2 + O(n^3) \tag{5.12}$$

Equation (5.12) defines the UV critical surface in the vicinity of the UVFP. The relevant eigendirection flows out of the fixed point and the irrelevant one runs into it. This is shown by the two oblique red lines in the phase diagram 5.2, which represents the renormalization group trajectories in a

domain close to the UV fixed point. In contrast to this fixed point, we see that the IRFP (represented by G in the figure) is attractive in all directions and, if we set one of the couplings to zero, the other becomes IR free. Those trajectories are represented by a horizontal and vertical red line flowing into G.

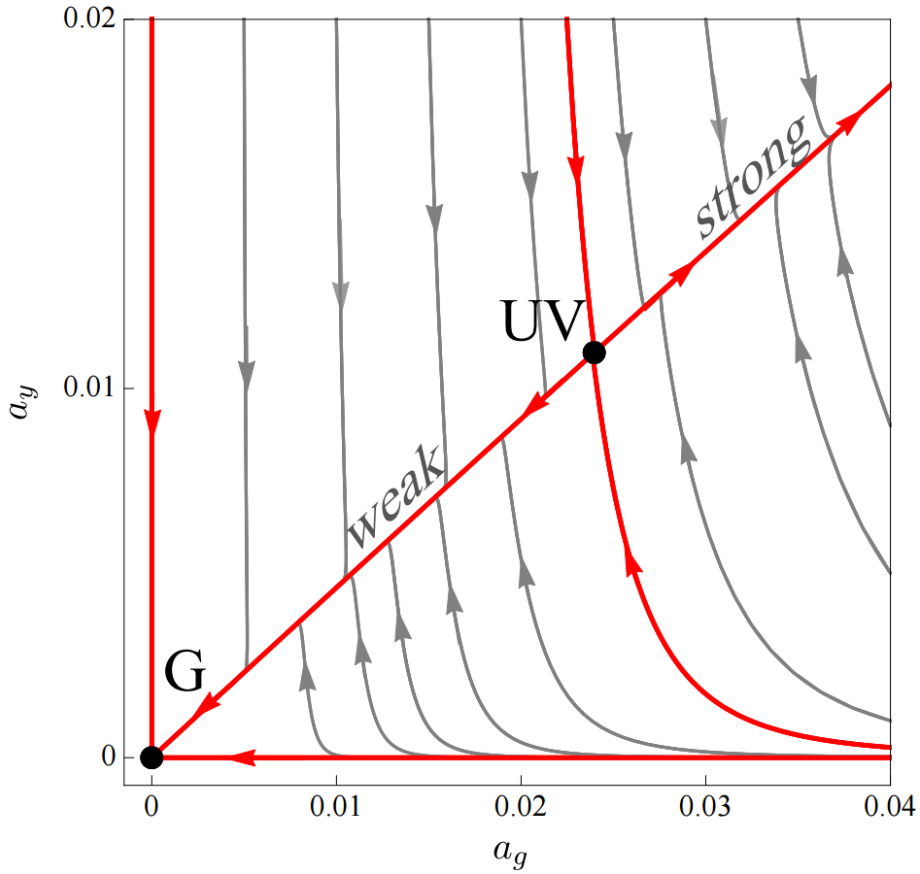

Figure 5.2: Phase diagram for the gauge-Yukawa renormalization group trajectories showing a IRFP (G) and a UVFP (UV). Figure adapted from [2].

Several further consistency issues are discussed in [2]. Firstly, stability holds for higher-order corrections (including scalar field dynamics, as mentioned before); in the sense that the leading order coefficients in n of the non-trivial fixed point (5.8), and of the irrelevant eigenvalue ϑ_2 (5.10a), remain unchanged when regarding higher-order gauge-Yukawa interactions and one-loop scalar interactions. For the relevant eigenvalue ϑ_1 the same fact holds for the first two coefficients. Therefore, the authors also expect stability in higher-power coefficients of n when including higher-order loop terms in the expansion.

Secondly, the authors refer to [22] in order to state that Weyl consistency

conditions are fulfilled by this model. Such conditions constraint the stability matrix expressed in terms of the un-squared coupling constants $(g_i) = (g, y)$ in the following way:

$$\frac{\partial \beta_i}{\partial g_j} = \frac{\partial \beta_j}{\partial g_i}$$

where $\beta_i = \mathrm{d}g_i/\mathrm{d}\log(p/\mu)$. These conditions symmetrize the stability matrix and can be used to define a metric χ^{ij} in a coupling space through the relation $\beta^i = \chi^{ij}\beta_j$. Such metric is an explicit result of [22].

Lastly, and without showing much detail, it is worth commenting that, in the expansion including scalar interactions, two UV fixed points are also found which are free of Landau poles, thus avoiding triviality and indicating that this scalars degrees of freedom may actually be fundamental. In this avoidance of triviality, the presence of gauge fields plays a crucial role. The mixing of the three types of fields helps the way out of triviality bounds.

6 Conclusion

In this paper we have addressed the three conventional limits concerning N and N_f and shown several properties of non-Abelian gauge theories in said limits. We focused as well on the effect of varying spacetime dimensionality in sections 2.3, 3 and 4.3. We reviewed 't Hooft limit, the dominance of planar diagrams, and understood the relation between two-particle states and Regge trajectories in QCD_2. We then proved that no physical fixed points can exist in QCD as a consequence of the ϵ-expansion as opposed to QED. We also gave an insight of how the screening effect extinguishes of the IRFP and how, by constraining the theory to dimensions $d < 3 + 1$, the IRFP is amplified. In section 4 we exhaustively studied the different possible behaviors the beta function can display from its second derivative and used the analysis to check the consistency with the previous conclusions. Finally, we found out UVFP can exist in $d = 3 + 1$ when including Yukawa interactions and the corresponding coupling. We showed this fixed point had a relevant and an irrelevant eigendirections which implied a critical surface could be defined in its vicinity. This sets the procedure to include scalar interactions (and higher-order expansion of the beta functions), such that triviality is avoided via asymptotic safety and, thus, could be considered fundamental.

References

[1] Lorenzo Di Pietro, Zohar Komargodski, Itamar Shamir, and Emmanuel Stamou. Quantum electrodynamics in d= 3 from the epsilon-expansion. *arXiv preprint arXiv:1508.06278*, 2015.

[2] Daniel F Litim and Francesco Sannino. Asymptotic safety guaranteed. *arXiv preprint arXiv:1406.2337*, 2014.

[3] Gerardus 't Hooft. A planar diagram theory for strong interactions. *Nucl. Phys. B*, 72(CERN-TH-1786):461–473, 1973.

[4] José Edelstein. Notes on string theory, April 2013.

[5] Marcos Mariño. *Instantons and Large N: An Introduction to Non-Perturbative Methods in Quantum Field Theory*. Cambridge University Press, 2015.

[6] Biagio Lucini and Marco Panero. Gauge theories at large n. *Physics Reports*, 526(2):93–163, 2013.

[7] Marco Bochicchio. Glueball and meson spectrum in large-n massless qcd. *arXiv preprint arXiv:1308.2925*, 2013.

[8] Gerard 't Hooft. A two-dimensional model for mesons. *Nuclear Physics B*, 75:461–470, 1974.

[9] Yuri V Kovchegov and Eugene Levin. *Quantum chromodynamics at high energy*. Cambridge University Press, 2012.

[10] Walter Greiner and Joachim Reinhardt. *Quantum electrodynamics*. Springer Science & Business Media, 2008.

[11] Vadim Kaplunovsky. Lecture notes on renormalization scheme dependence and minimal substraction, May 2016.

[12] Michael Peskin and Dan Schroeder. An introduction to quantum field theory. 1995.

[13] T Van Ritbergen, JAM Vermaseren, and SA Larin. The four-loop β-function in quantum chromodynamics. *Physics Letters B*, 400(3):379–384, 1997.

[14] JA Gracey. The qcd β-function at o (1nf). *Physics Letters B*, 373(1):178–184, 1996.

[15] Julian Schwinger. Gauge invariance and mass. ii. *Physical Review*, 128(5):2425, 1962.

[16] A Casher, J Kogut, and Leonard Susskind. Vacuum polarization and the absence of free quarks. *Physical Review D*, 10(2):732, 1974.

[17] AL Kataev and VS Molokoedov. Fourth-order qcd renormalization group quantities in the v scheme and the relation of the β function to the gell-mann–low function in qed. *Physical Review D*, 92(5):054008, 2015.

[18] Gerard 't Hooft. Probing the small distance structure of canonical quantum gravity using the conformal group. *arXiv preprint arXiv:1009.0669*, 2010.

[19] Marie E Machacek and Michael T Vaughn. Two-loop renormalization group equations in a general quantum field theory:(i). wave function renormalization. *Nuclear Physics B*, 222(1):83–103, 1983.

[20] Marie E Machacek and Michael T Vaughn. Two-loop renormalization group equations in a general quantum field theory (ii). yukawa couplings. *Nuclear Physics B*, 236(1):221–232, 1984.

[21] Marie E Machacek and Michael T Vaughn. Two-loop renormalization group equations in a general quantum field theory:(iii). scalar quartic couplings. *Nuclear Physics B*, 249(1):70–92, 1985.

[22] Oleg Antipin, Marc Gillioz, Esben Mølgaard, and Francesco Sannino. The a theorem for gauge-yukawa theories beyond banks-zaks fixed point. *Physical Review D*, 87(12):125017, 2013.